Cosmological Constraints on Higgs-Dilaton Inflation

Manuel Trashorras

Instituto de Física Teórica,
Universidad Autónoma de Madrid,
Cantoblanco 28049 Madrid, Spain.

Cosmic Microwave Background, Large Scale Structure and 21 cm Surveys Workshop, June 2016

Outline

The present presentation is an overview of arXiv:1604.06760v2

Cosmological Constraints on Higgs-Dilaton Inflation

Manuel Trashorras,* Savvas Nesseris,† and Juan García-Bellido‡

Instituto de Física Teórica UAM-CSIC, Universidad Autonóma de Madrid, Cantoblanco, 28049 Madrid, Spain

We test the viability of the Higgs-Dilaton model (HDM) compared to the evolving Dark Energy ($w_0 w_a$CDM) model, in which the cosmological constant model ΛCDM is also nested, by using the latest cosmological data that includes the Cosmic Microwave Background temperature, polarization and lensing data from the *Planck* satellite (2015 data release), the BICEP and Keck Array experiments, the Type Ia supernovae from the JLA catalog, the Baryon Acoustic Oscillations from CMASS, LOWZ and 6dF, the Weak Lensing data from the CFHTLenS survey and the Matter Power Spectrum measurements from the SDSS (data release 7). We find that the values of all cosmological parameters allowed by the Higgs-Dilaton model Inflation are well within the *Planck* satellite (2015 data release) constraints. In particular, we have that $w_0 = -1.0001^{+0.0072}_{-0.0074}$, $w_a = 0.00^{+0.15}_{-0.16}$, $n_s = 0.9693^{+0.0083}_{-0.0082}$, $\alpha_s = -0.001^{+0.013}_{-0.014}$ and $r_{0.05} = 0.0025^{+0.0017}_{-0.0016}$ (95.5%C.L.). We also place new stringent constraints on the couplings of the Higgs-Dilaton model and we find that $\xi_\chi < 0.00328$ and $\xi_h/\sqrt{\lambda} = 59200^{+30000}_{-20000}$ (95.5%C.L.). Furthermore, we report that the HDM is at a slightly better footing than the $w_0 w_a$CDM model, as they both have practically the same *chi-square*, i.e. $\Delta\chi^2 = \chi^2_{w_0 w_a \mathrm{CDM}} - \chi^2_{\mathrm{HDM}} = 0.18$, but with the HDM model having two parameters less, and finally a Bayesian evidence favoring equally the two models but the HDM being preferred by the AIC and DIC information criteria.

Main features

The Higgs-Dilaton Model (see García-Bellido et al., 2011) has

Two main ingredients:

1. Non-minimal extension of the Standard Model (SM) to gravity.
2. Replacement of General Relativity (GR) with Unimodular Gravity (UR).

Two main features:

1. By construction, classically scale-invariant (SI).
2. Scales G, v and Λ originate from the spontaneous symmetry breaking of SI.

The Higgs-Dilaton Model can explain inflation and present-day cosmological acceleration from slow-roll of the fields.

Higgs-Dilaton Model Lagrangian

In the Jordan frame (JF), the HDM Lagrangian is

$$
\begin{aligned}
\frac{\mathcal{L}_{SI+UG,JF}}{\sqrt{-\hat{g}}} =& \frac{1}{2}\left(\xi_\chi \chi^2 + \xi_h h^2\right)\hat{R} + K.T. \\
& - \left(\lambda\left(\frac{1}{2}h^2 - \frac{\alpha}{2\lambda}\chi^2\right)^2 + \beta\chi^4 - \Lambda_0\right)
\end{aligned} \tag{1}
$$

Moving to the Einstein frame (EF) , the HDM Lagrangian is

$$
\frac{\mathcal{L}_{SI+UG,EF}}{\sqrt{-\tilde{g}}} = M_P^2 \frac{\widetilde{R}}{2} + N.C.K.T. \tag{2}
$$

$$
- \frac{M_P^4\left(\frac{\lambda}{4}\left(h^2 - \frac{\alpha}{\lambda}\chi^2\right)^2 + \beta\chi^4 + \Lambda_0\right)}{\left(\xi_\chi\chi^2 + \xi_h h^2\right)^2} \tag{3}
$$

The ground states are, depending on β,

$$
h_0^2 = \frac{\alpha}{\lambda}\chi_0^2 + \frac{4\beta\xi_h\chi_0^2}{\lambda\xi_\chi + \alpha\xi_h} \tag{4}
$$

Slow-roll parameters

For the homogeneous background we take the usual homogeneous and isotropic FRWL metric,

$$ds^2 = \tilde{g}_{\mu\nu} dx^\mu dx^\nu = -dt^2 + a^2(t) d\vec{x}^2 \qquad (5)$$

We introduce the slow roll (SR parameters, which verify $\epsilon, \eta = |\boldsymbol{\eta}| < 1$ during inflation.

$$\epsilon \equiv -\frac{H'}{H} = \frac{1}{2}\frac{|\phi'|^2}{M_P^2} \quad \text{and} \quad \boldsymbol{\eta} \equiv \frac{1}{|\phi'|}\frac{\mathrm{D}\phi'}{\mathrm{dN}} \qquad (6)$$

Working with the number of e-folds $N \equiv \ln a \simeq e^{Ht}$ and renaming the fields $(\phi^1, \phi^2) = (\chi, h)$, the Friedmann and Klein-Gordon equations are well approximated by

$$H^2 = \frac{\tilde{U}}{3M_P^2} \quad \text{and} \quad \phi' = -\mathrm{M_P^2} \boldsymbol{\nabla}^\dagger \ln \tilde{\mathrm{U}} \qquad (7)$$

Slow-roll and reheating

Redefining the fields ($A_i \equiv 1 + 6\xi_i,\ i = h, \chi$)

$$\rho = \frac{M_P}{2} \ln\left(\frac{A_\chi \chi^2 + A_h h^2}{M_P^2}\right) \rightarrow \rho' = 0 \tag{8}$$

$$\theta = \tan^{-1}\left(\sqrt{\frac{A_h}{A_\chi}}\frac{h}{\chi}\right) \rightarrow \theta' = -\frac{4\xi_\chi}{A_\chi}\cot\theta\left(1 + \frac{6\xi_\chi\xi_h}{\kappa(\theta)}\right) \tag{9}$$

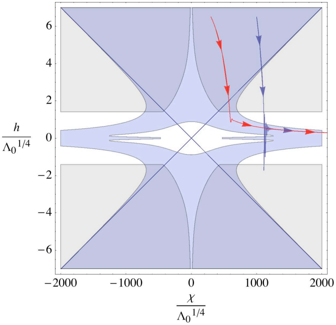

Figure: Blue: SR region. Shaded: SI region. Red trajectories oscillate a few times and don't reheat. Blue trajectories fast-roll towards the potential valley, oscillate strongly and reheat. Fig. from García-Bellido et al., 2011.

Power spectrum of perturbations

Including scalar and tensor perturbations in the Newtonian transverse traceless gauge (see Mukhanov et al., 1990),

$$ds^2 = -(1+2\Phi)\,dt^2 + a(t)^2\left((1-2\Psi)\,\delta_{ij} + h_{ij}^{TT}\right)dx^i dx^j \tag{10}$$

where Φ and Ψ are the Bardeen potentials.

The primordial scalar (curvature) perturbation

$$\zeta \equiv \Psi - \frac{H}{\dot{H}}\left(\dot{\Psi} + H\Phi\right) . \tag{11}$$

is conserved if inflation takes place in the scale invariant region.

The scalar and tensor power spectra are (at at $a^* H = k_0$)

$$\mathcal{P}_s(k) \simeq \frac{1}{2M_P^2\epsilon}\left(\frac{H^*}{2\pi}\right)^2 \quad \text{and} \quad \mathcal{P}_t(k) \simeq \frac{8}{M_P^2}\left(\frac{H^*}{2\pi}\right)^2 \tag{12}$$

Scalar and Tensor Power Spectrum

Using redefined slow roll parameters: the speed-up $\eta_{||}$ and the turn $\eta_{\perp}$ rate, (see García-Bellido et al., 2011).)

Scalar power spectrum

$$n_s(k) \equiv 1 + \frac{d \ln \mathcal{P}_s}{d \ln k} \quad (13)$$

$$\simeq 1 - 2(\epsilon + \eta_{||}) \quad (14)$$

$$\alpha_s \equiv dn_s/d \ln k \quad (15)$$

$$\simeq -(2\epsilon + \xi)2\eta_{||} \quad (16)$$

Tensor power spectrum

$$n_t(k) \equiv \frac{d \ln \mathcal{P}_t}{d \ln k} \quad (17)$$

$$\simeq -2\epsilon \quad (18)$$

$$\alpha_t \equiv dn_t/d \ln k \quad (19)$$

$$\simeq 0 \quad (20)$$

Tensor to scalar ratio and the inflation consistency condition:

$$r \equiv \frac{A_t}{A_s} \simeq 16\epsilon \quad \text{and} \quad \mathrm{r} = -8\mathrm{n}_\mathrm{t} \quad (21)$$

Scalar and Tensor Power Spectrum

The scalar power spectrum parameters depend on

$$A_s(k_0) \simeq \frac{\lambda \sinh^2(4\xi_\chi N^*)}{1152\pi^2\xi_\chi^2\xi_h^2} \tag{22}$$

$$n_s(k_0) \simeq 1 - 8\xi_\chi \coth(4\xi_\chi N^*) \tag{23}$$

$$\alpha_s(k_0) \simeq -32\xi_\chi^2 \sinh^{-2}(4\xi_\chi N^*) \tag{24}$$

The tensor-to-scalar ratio gives both $A_t(k_0)$ and $n_t(k_0)$,

$$r(k_0) = -8n_t(k_0) \simeq 192\xi_\chi^2 \sinh^{-2}(4\xi_\chi N^*) \tag{25}$$

A consistency check for the Higgs-Dilaton Model is found:

$$\alpha_s(k_0) \simeq -\frac{1}{6}\,r(k_0) = \frac{4}{3}\,n_t(k_0) \tag{26}$$

Moving towards the DE Era

After reheating, the scalar fields settle down in one of the potential valleys $h(t)^2 \simeq \frac{\alpha}{\lambda}\chi(t)^2$. Moving to new variables:

$$\tilde{\rho} = \rho\gamma^{-1} \quad , \quad \tilde{\theta} = \frac{\mathrm{M_P}}{\mathrm{a}} \tanh^{-1}\left(\sqrt{1-\varsigma}\,\cos\theta\right) \tag{27}$$

with the parameters

$$a = \sqrt{\frac{\xi_\chi(1-\zeta}{\zeta}} \quad \text{and} \quad \gamma = \sqrt{\frac{\xi_\chi}{1+6\xi_\chi}} \tag{28}$$

The ground states become

$$\tanh^2(a\,\tilde{\theta}(t)/M_P) \simeq \frac{1-\varsigma}{1+\frac{\alpha}{\lambda}\frac{1+6\xi_h}{1+6\xi_\chi}} = 1-\varsigma \tag{29}$$

Quintessence run-away potential

Plugging the ground states into the EF Lagrangian

$$\frac{\mathcal{L}}{\sqrt{-\tilde{g}}} \simeq \frac{M_P^2}{2}\tilde{R} - \frac{1}{2}(\partial\tilde{\rho})^2 - \tilde{V}_{QE}(\tilde{\rho}) \tag{30}$$

we get a run-away-type potential

$$\tilde{V}_{QE}(\tilde{\rho}) = \frac{\Lambda_0}{\gamma^4} e^{-4\gamma\tilde{\rho}/M_P} \tag{31}$$

of the kind proposed for QE. (see Saposhnikov et al., 2008). This allows the dilaton field to play the role of a dynamic DE.

Equations of motion

The equation of motion for the homogeneous field $\tilde{\rho}(t)$ is

$$\ddot{\tilde{\rho}} + 3H\dot{\tilde{\rho}} + \frac{dV_{QE}}{d\tilde{\rho}} = 0 \tag{32}$$

or, equivalently, the equation of motion of dark energy density is

$$\dot{\varrho}_{QE} = -3H\varrho_{QE}\left(1 + w_{QE}\right) \tag{33}$$

and rewriting in terms of $\delta_{QE} \equiv 1 + w_{QE}$, taking into account the cosmic sum rule, and w.r.t. the e-folds,

$$\delta'_{QE} = -3\delta_{QE}(2-\delta_{QE}) + 4\gamma(2-\delta_{QE})\sqrt{3\delta_{QE}\Omega_{QE}} \tag{34}$$

$$\Omega'_{QE} = 3(\delta_b - \delta_{QE})\Omega_{QE}(1-\Omega_{QE}) \tag{35}$$

where sub-index "b" stands for any matter fluid,

Field trajectories

For $0 \leq \delta_b \leq 2$, the trajectories approach one of two attractor solutions, depending on γ:

1. If $4\gamma > \sqrt{3\delta_b}$, the scalar field has $w_{QE} = 1$.
2. If $4\gamma < \sqrt{3\delta_b}$, the scalar has $w_{QE} = 16\gamma^2/3 - 1 < -1/3$.

For $\xi_\chi < 1/2$, we are assured that w_{QE} is driven to the second attractor. Therefore

1. Eventually Ω_{QE} becomes relevant.
2. The scalar fields $\tilde{\rho}$ start rolling down the valleys.
3. δ_{QE} starts growing towards its attractor value.
4. Accelerated expansion of space begins.

Constraint relations

For $\delta_{QE} \ll 1$, the E.o.M. yield (see Scherrer et al., 2007)

$$\delta_{QE} \simeq \frac{16\gamma^2}{3}\left[F(\Omega_{QE})\right]^2 \simeq \frac{8}{3}\frac{\xi_\chi}{1+6\xi_\chi} \tag{36}$$

$$F(\Omega_{QE}) = \frac{1}{\sqrt{\Omega_{QE}}} - \frac{1}{2}\left(\frac{1}{\Omega_{QE}} - 1\right)\ln\frac{1+\sqrt{\Omega_{QE}}}{1-\sqrt{\Omega_{QE}}} \tag{37}$$

Now $n_s(k_0)$ and $\delta^0_{QE}(a)$ are given in terms of ξ_χ and/or N^*

$$-3\delta_{DE} \simeq n_s - 1 \quad , \quad 3\mathrm{w}^{\mathrm{a}}_{\mathrm{DE}} \simeq \alpha_s \tag{38}$$

which can be equivalently written in differential form

$$\left.\frac{d\ln\varrho_{\mathrm{QE}}}{d\ln a}\right|_{a^*} \simeq \left.\frac{d\ln P_s(k)}{d\ln k}\right|_{k_0} \quad , \quad \left.\frac{\mathrm{d}^2\ln\varrho_{\mathrm{DE}}}{(\mathrm{d}\ln \mathrm{a})^2}\right|_{\mathrm{a}^*} \simeq \left.\frac{\mathrm{d}^2\ln\mathcal{P}_{\mathrm{s}}(\mathrm{k}))}{(\mathrm{d}\ln \mathrm{k})^2}\right|_{\mathrm{k}_0} \tag{39}$$

This may be understood as a consequence of scale invariance.

Note on COSMOMC modifications

The past calculations on the spectral quantities rely on a non-standard parametrization of the dark energy equation of state. We have to replace the one used by CAMB, within COSMOMC (see Lewis, 2002).

$$w_{DE} = w_0 + w_a(1-a) \quad \rightarrow \quad w_{DE} = w_0 + w_a \log(a/a_0) \tag{40}$$

Also, we have to replace the scalar and tensor power spectrum in CAMB with one calculated with the HDM constraints:

$$n_s = 1 - \frac{2}{N_{\mathrm{inf}}} G \coth G \tag{41}$$

$$\alpha_s = -\frac{8 w^a_{\mathrm{DE}} F}{3\delta_{\mathrm{DE}} N^2_{\mathrm{inf}}} G^2 \left(\mathrm{csch}^2 G - G \coth G^2\right) \tag{42}$$

$$r = \frac{12}{N^2_{\mathrm{inf}}} G^2 \mathrm{csch}^2 G \tag{43}$$

$$G = \frac{6\delta_{\mathrm{DE}} N_{\mathrm{inf}}}{8F(\Omega_{\mathrm{QE}}) - 9\delta_{\mathrm{DE}}} \tag{44}$$

Overview of the MCMC output

For the $w_0 w_a$CDM run (Planck+Lensing+BAO+WL+MPK+JLA):

- we have 16 chains in total,
- each cut at 20k samples (after burn-in),
- adding up to 320k samples in total.

For the HMD run (Planck+Lensing+BAO+WL+MPK+JLA):

- we have 32 chains in total,
- each cut at 16k samples (after burn-in),
- adding up to 515k samples in total.

Cosntrains on cosmological parameters

Parameter	$w_0 w_a$CDM	HDM (pred.)	HDM (obs.)
		Confidence level 95.5%	
$\Omega_b h^2$	$0.02237^{+0.00051}_{-0.00049}$	$0.02231^{+0.00043}_{-0.00043}$	$0.02233^{+0.00044}_{-0.00043}$
$\Omega_c h^2$	$0.1177^{+0.0035}_{-0.0035}$	$0.1181^{+0.0024}_{-0.0021}$	$0.1177^{+0.0025}_{-0.0025}$
$100\theta_{MC}$	$1.04111^{+0.00088}_{-0.00088}$	$1.04106^{+0.00080}_{-0.00081}$	$1.04110^{+0.00083}_{-0.00082}$
τ_{RE}	$0.069^{+0.038}_{-0.035}$	$0.066^{+0.025}_{-0.025}$	$0.070^{+0.027}_{-0.027}$
$\ln(10^{10} A_s)$	$3.067^{+0.069}_{-0.064}$	$3.063^{+0.049}_{-0.049}$	$3.068^{+0.050}_{-0.050}$
w_0	$-0.93^{+0.21}_{-0.20}$	$-0.99999^{+0.0056}_{-0.0060}$	$-1.0001^{+0.0072}_{-0.0074}$
w_a	$-0.21^{+0.69}_{-0.74}$	$-0.02^{+0.18}_{-0.22}$	$0.00^{+0.15}_{-0.16}$
n_s	$0.969^{+0.011}_{-0.011}$	$0.9665^{+0.0045}_{-0.0051}$	$0.9693^{+0.0083}_{-0.0082}$
α_s	$-0.005^{+0.015}_{-0.015}$	$-0.003^{+0.015}_{-0.014}$	$-0.001^{+0.013}_{-0.014}$
$r_{0.05}$	< 0.0964	$0.0002^{+0.0031}_{-0.0033}$	$0.0025^{+0.0017}_{-0.0016}$
$N_{\rm inf}$	n/a	n/a	70^{+20}_{-20}

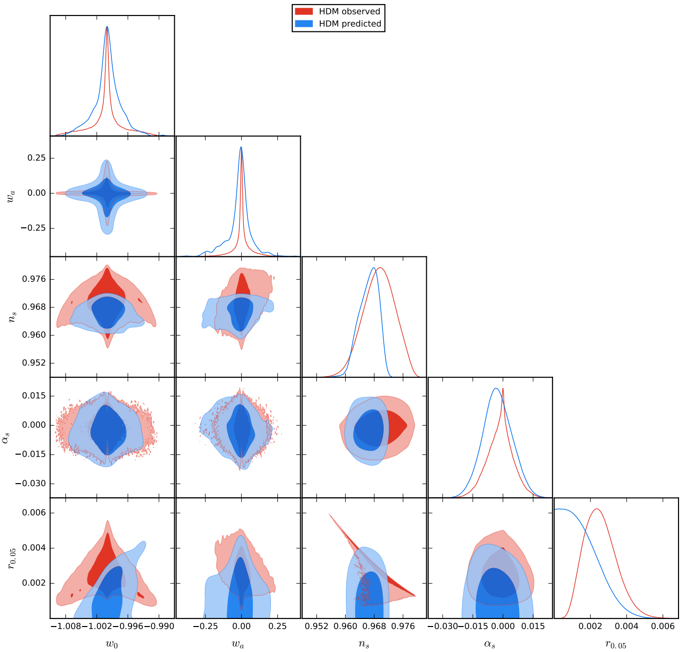
HDM observed
HDM predicted
w_a
n_s
α_s
$r_{0.05}$
w_0
w_a
n_s
α_s
$r_{0.05}$
0.25
0.00
−0.25
0.976
0.968
0.960
0.952
0.015
0.000
−0.015
−0.030
0.006
0.004
0.002
−1.008 −1.002 −0.996 −0.990
−0.25 0.00 0.25
0.952 0.960 0.968 0.976
−0.030 −0.015 0.000 0.015
0.002 0.004 0.006

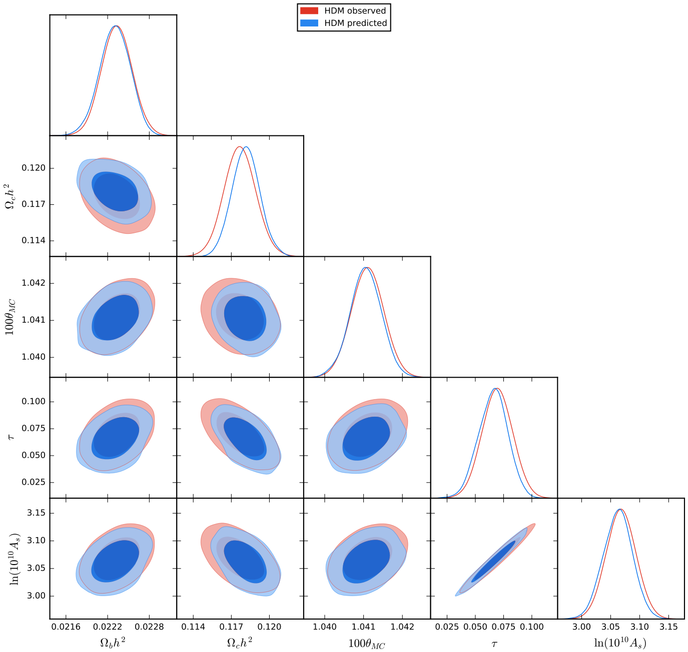
HDM observed
HDM predicted
$\Omega_c h^2$
0.120
0.117
0.114
$100\theta_{MC}$
1.042
1.041
1.040
τ
0.100
0.075
0.050
0.025
$\ln(10^{10}A_s)$
3.15
3.10
3.05
3.00
0.0216 0.0222 0.0228
$\Omega_b h^2$
0.114 0.117 0.120
$\Omega_c h^2$
1.040 1.041 1.042
$100\theta_{MC}$
0.025 0.050 0.075 0.100
τ
3.00 3.05 3.10 3.15
$\ln(10^{10}A_s)$

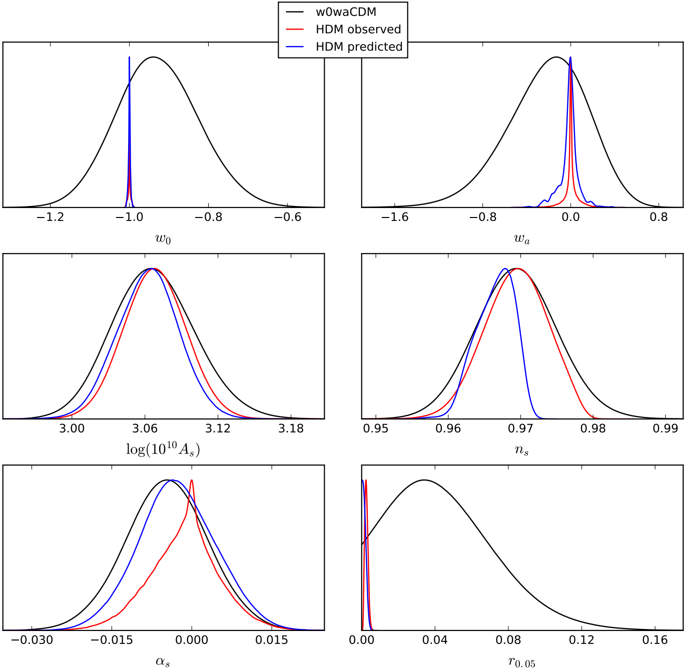
w0waCDM
HDM observed
HDM predicted
−1.2
−1.0
−0.8
−0.6
w_0
−1.6
−0.8
0.0
0.8
w_a
3.00
3.06
3.12
3.18
$\log(10^{10}A_s)$
0.95
0.96
0.97
0.98
0.99
n_s
−0.030
−0.015
0.000
0.015
α_s
0.00
0.04
0.08
0.12
0.16
$r_{0.05}$

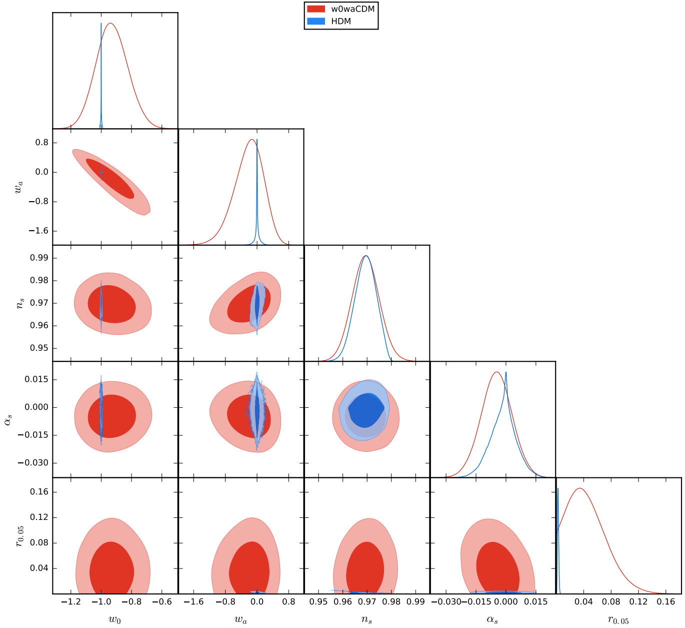
w0waCDM
HDM
w_0
w_a
n_s
α_s
$r_{0.05}$
−1.2 −1.0 −0.8 −0.6
−1.6 −0.8 0.0 0.8
0.95 0.96 0.97 0.98 0.99
−0.030 −0.015 0.000 0.015
0.04 0.08 0.12 0.16

Figures of Merit

FoM	$w_0 w_a$CDM	HDM	$Q_{w_0 w_a \mathrm{CDM,HDM}}$
$w_0\,,\,w_a$	8	2216	272
$w_0\,,\,A_s$	40	3014	76
$w_0\,,\,n_s$	240	17847	74
$w_0\,,\,\alpha_s$	170	12281	72
$w_0\,,\,r_{0.05}$	50	99458	1985
$w_a\,,\,A_s$	13	157	12
$w_a\,,\,n_s$	74	940	13
$w_a\,,\,\alpha_s$	49	635	13
$w_a\,,\,r_{0.05}$	14	5152	358
$A_s\,,\,n_s$	956	1405	1.5
$A_s\,,\,\alpha_s$	559	946	1.7
$A_s\,,\,r_{0.05}$	156	7334	47
$n_s\,,\,\alpha_s$	3202	5424	1.7
$n_s\,,\,r_{0.05}$	951	213009	224
$\alpha_s\,,\,r_{0.05}$	698	28838	41

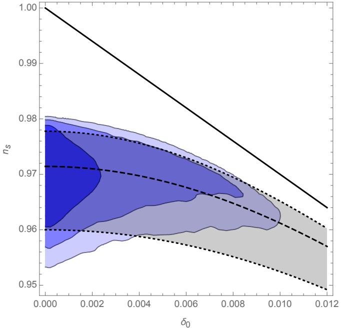
1.00
0.99
0.98
0.97
0.96
0.95
n_s
0.000
0.002
0.004
0.006
0.008
0.010
0.012
δ_0

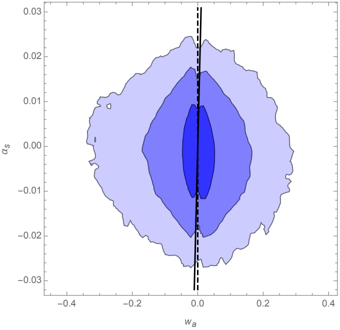
0.03
0.02
0.01
0.00
−0.01
−0.02
−0.03
α_s
−0.4
−0.2
0.0
0.2
0.4
w_a

Constraints on HDI couplings

We present the constraints for the HDM couplings $\xi_h/\sqrt{\lambda}$ and ξ_χ by numerically inverting Eqs. (22) and (23).

At the 95.5% confidence level, we find results in line with what was expected $\xi_\chi \mathcal{O}(10^{-3})$ and $\xi_h/\sqrt{\lambda}\mathcal{O}(10^5)$

$$\xi_\chi < 0.00328 \tag{45}$$

$$\xi_h/\sqrt{\lambda} = 59200^{+30000}_{-20000} \tag{46}$$

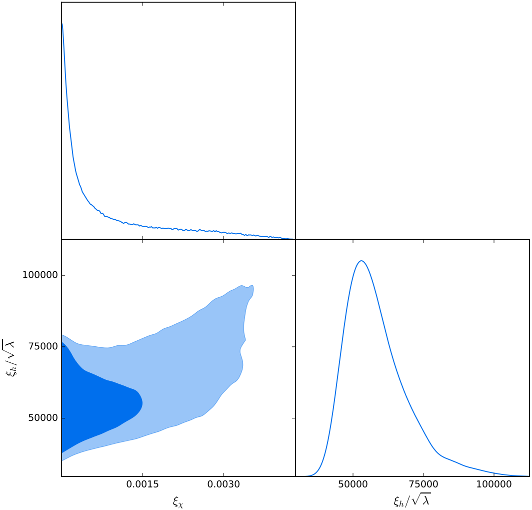
100000
75000
50000
$\xi_h/\sqrt{\lambda}$
0.0015
0.0030
ξ_χ
50000
75000
100000
$\xi_h/\sqrt{\lambda}$

Bayesian evidence

We find the HDM is on an equal footing w.r.t. the $w_0 w_a$CDM: they have a similar chi-square, i.e. $\Delta\chi^2 = \chi^2_{w_0 w_a \mathrm{CDM}} - \chi^2_{\mathrm{HDM}} = 0.178$, but with the HDM model having two fewer parameters.

We also compare the two models and compare them by making use of the Jeffreys' scale. The Bayesian evidence is defined as

$$E(\mathbf{D}|\mathcal{M}) = \int_{\mathcal{R}} du\ \mathcal{L}(\mathbf{D}|u,\mathcal{M})\pi(u,\mathcal{M}) \tag{47}$$

We make use of three methods for the Bayesian analysis

$$E^{\mathrm{HMA}}(\mathbf{D}|\mathcal{M}) = \left(\frac{1}{N}\sum_{i=1}^{N}\frac{1}{\mathcal{L}(\mathbf{D}|u,\mathcal{M})}\right)^{-1} \tag{48}$$

$$\mathrm{AIC}(\mathbf{D}|\mathcal{M}) = 2k + \chi^2_{\min}(\mathbf{D}|u,\mathcal{M}) \tag{49}$$

$$\mathrm{DIC}(\mathbf{D}|\mathcal{M}) = 2\langle\chi^2(\mathbf{D}|u,\mathcal{M})\rangle - \chi^2_{\min}(\mathbf{D}|u,\mathcal{M}) \tag{50}$$

HMA, AIC and DIC results

We find the Bayesian evidence ratios and AIC/BIC differences for HDM and $w_0 w_a$CDM to be

$$R^{\mathrm{HMA}}_{\mathrm{HDM},w_0 w_a\mathrm{CDM}} = 0.55 \approx 1.8^{-1} \tag{51}$$

$$\Delta\mathrm{AIC}_{\mathrm{HDM},w_0 w_a\mathrm{CDM}} = -4.2, \tag{52}$$

$$\Delta\mathrm{DIC}_{\mathrm{HDM},w_0 w_a\mathrm{CDM}} = -3.5\ , \tag{53}$$

which imply that the HDM and t$w_0 w_a$CDM are more or less on an equal footing as seen by the evidence ratio R, but have the HDM somewhat disfavoured in Jeffrey's scale by the ΔAIC and ΔDIC. The three are, though, very rough approximations.

Conclusions

- No tension is found between the Higgs-Dilaton Model and current observations within $w_0 w_a \Lambda$CDM.
- The Higgs-Dilaton Model puts very stringent bounds on w_0, w_a and r. To a lesser extent, also on α_S.
- Some of the contours for combinations of these parameters exhibit very non-gaussian shapes.
- Bounds for r and w_0 in particular should be able to accept or exclude the model in the near future.